論 文

Simulation of Mold Fluid Flow

Jong-Hyun Kim*, In-Cheol Lim**, Sung-Sik Kim***

주조시 비정상 유동에 대한 수치해석

김 종 현*, 임 인 철**, 김 성 식***

초 록

주조시 주형내의 유동해석을 위해서는 시간에 따라 변화하는 자유표면 위치에 대한 정확한 정보가 요구되는 관계로 난제로 여겨져 왔다. 따라서 대부분의 연구는 초기치 속도를 정의하기 위해서 순간충입(instantaneous filling)을 가정하여 수치 해석을 하였던 것이다.

본 연구는 Modified Solution Algorithm-Volume of Fluid Method (MSOLA-VOF)를 개발하는 주조시 주형내의 유동을 수치적으로 해석하며, 유속이 수평 주조, 수직 주조의 경우에 어떤 영향을 미치는가에 대하여 연구하였다. 결론으로 응고 연구에 있어서 초기의 순간충입은 비현실적인 가정이라는 것이 밝혀졌으며, 충입시 초기 속도 분포와 결정 생성은 밀접한 관계가 있음을 알 수 있었다.

1. Introduction

A mathematically correct treatment of the free surface movements is a central issue of many practical engineering problems. One of the typical examples can be found in the area of mold filling process. This process, due to highly transient movements of molten material, results in a significant effect on the characteristic of the castified material.

Most existing numerical algorithms which handle the latent heat release during the solidification process are derived on the basis of the instantaneous filling assumption[1-6]. The molten materials are assumed to instantaneously fill the mold and, thus, there is no motion of the fluid at the beginning of the solidification process. But it is obvious that the mold filling process is highly transient fluid flow phenomenon.

Several codes describing the free surface problems are presently available. Marker-Cell(MAC) technique[7] and its derevatives, Simplified Marker-Cell (SMAC) technique [8] and Solution Algorithm-Volume of Fluid (SOLA-VOF)[9-12], all treat the free surface fluid flow problems. All of these numerical codes are basically finite difference schemes for the mathematical analysis of the fluid flow problem. In these codes, the domain is divided into a number of subdomains which are called cells. Then, the set of fluid function values (F) are introduced as a system to represent the fluid domain at that instant.

* Research Engineer(Ph.D.), School of Mechanical Eng.

** Graduate Student, School of Eng., Science and Mechanics, G.I.T., Atlanta Ga. 30332, U.S.A.(미국 조지아 공과대)

*** Assistant Professor(Ph.D.), Department of Inorganic Materials Eng., Hong Ik University.(홍익대 무기재료공학과)

With the application of fluid dynamics principles, the velocity field of the moving domain can be calculated. Next, the fluid function value (F) is adjusted in accordance with the velocity field just obtained.

The modified Solution Algorithm-Volume of Fluid Method(MSOLA-VOF) is intrduced in this paper. The penalty function approach is used to minimize the CPU time requirement by eliminating the dependent variable. Two cases are presented to demonstrate the effect of velocity and free surface movements during the filling process.

2. Finite Difference Formulations of Governing Equations

To understand free surface movements, the continuity equation and the Navier-Stokes equations are solved in the region of interest. The continuity equation and the Navier-Stokes equations can be expressed repectively ;

$$\frac{\partial u}{\partial x}+\frac{\partial v}{\partial y}=0 \quad , \tag{1}$$

$$\frac{\partial u}{\partial t}+u\frac{\partial u}{\partial x}+v\frac{\partial u}{\partial y}=-\frac{1}{\rho}\frac{\partial P}{\partial x}+g_x +\nu\left(\frac{\partial^2 u}{\partial x^2}+\frac{\partial^2 u}{\partial y^2}\right) \quad , \tag{2}$$

$$\frac{\partial v}{\partial t}+u\frac{\partial v}{\partial x}+v\frac{\partial v}{\partial y}=-\frac{1}{\rho}\frac{\partial P}{\partial y}+g_y +\nu\left(\frac{\partial^2 v}{\partial x^2}+\frac{\partial^2 v}{\partial y^2}\right) \quad , \tag{3}$$

Equations (1)－(3) are now discretized with respect to an Eulerian grid of fixed rectangular cells which is shown in Figure 1. The finite difference scheme of continuity equation is adapted to rectangular grid;

$$D_{i,j}=\frac{1}{\delta x}(u_{i+1/2,j}-u_{i-1/2,j})+\frac{1}{\delta y}(v_{i,j+1/2}-v_{i,j-1/2}) \tag{4}$$

Thus, the continuity equation should satisfy,

$$D_{i,j}=0 \quad , \tag{5}$$

for each cell at every time step.

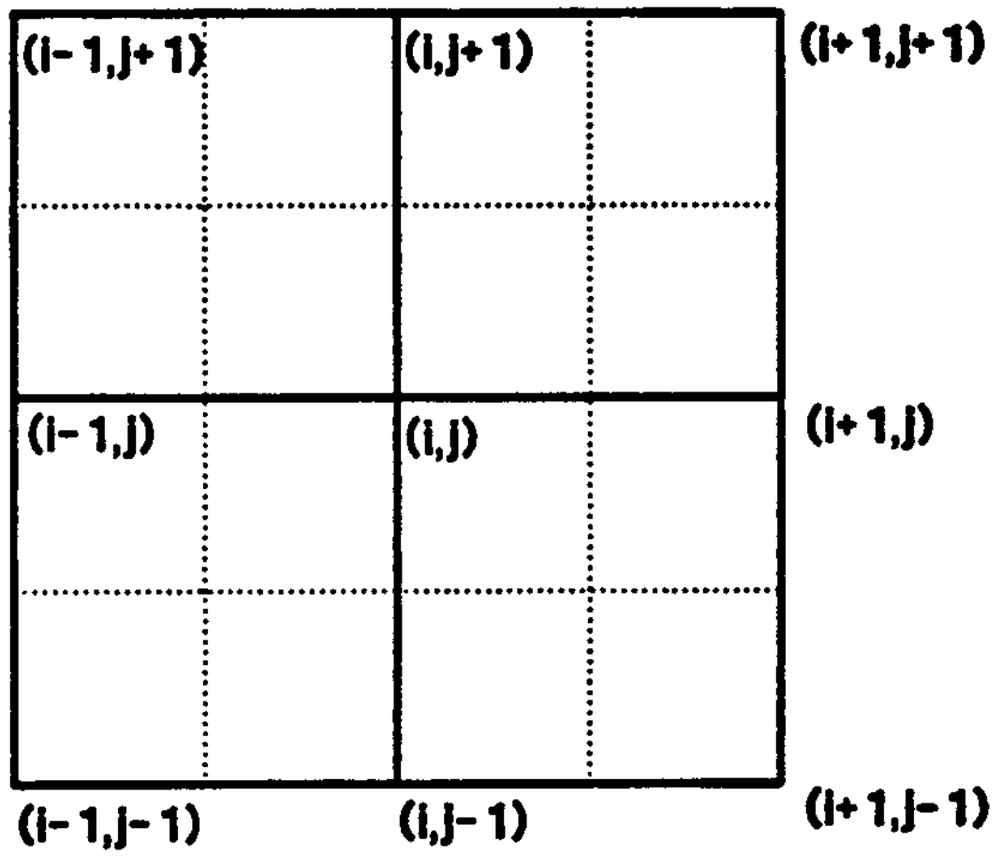

Figure 1. Location of dependent variables in the rectangular grid.

Using Taylor expansion, the finite difference form of the Navier-Stokes equations (2) and (3) are represented as;

$$\frac{1}{\delta t}(u^{n+1}_{i+1/2,j}-u_{i+1/2,j})=\frac{1}{\delta x}((u_{i,j})^2-(u_{i+1,j})^2) +\frac{1}{\delta y}((uv)_{i+1/2,j-1/2}-(uv)_{i+1/2,j+1/2}) +g_x+\frac{1}{\rho\delta x}(p_{i,j}-p_{i+1,j}) \quad , \tag{6}$$
$$+\nu\Big[\frac{1}{\delta x^2}(u_{i+3/2,j}+u_{i-1/2,j}-2u_{i+1/2,j}) +\frac{1}{\delta y^2}(u_{i+1/2,j+1}+u_{i+1/2,j-1}-2u_{i+1/2,j})\Big]$$

$$\frac{1}{\delta t}(v^{n+1}_{i,j+1/2}-v_{i,j+1/2})=\frac{1}{\delta x}((uv)_{i-1/2,j+1/2} -(uv)_{i+1/2,j+1/2}) +\frac{1}{\delta y}((v_{i,j})^2-(v_{i+1/2,j+1/2})^2) +g_x+\frac{1}{\rho\delta y}(p_{i,j}-p_{i,j+1}) \quad . \tag{7}$$
$$+\nu\Big[\frac{1}{\delta x^2}(v_{i+1,j+1/2}+v_{i-1,j+1/2}-2v_{i,j+1/2}) +\frac{1}{\delta y^2}(v_{i,j+3/2}+v_{i,j-1/2}-2v_{i,j+1/2})\Big]$$

The superscript $n+1$ refers to a value at time $(n+1)\delta t$, so that n counts the number of cycles. For simplicity, superscript n is omitted in each term where n is not shown. The undefined quantities in equations (6)

and (7) are specified by using a simple average in the adjacent quantities. For examples,

$$u_{i,j}=\frac{1}{2}(u_{i+1/2,j}+u_{i-1/2,j})$$
$$v_{i,j}=\frac{1}{2}(v_{i,j+1/2}+v_{i,j-1/2})$$
$$u_{i+1/2,j+1/2}=\frac{1}{2}(u_{i+1/2,j}+u_{i+1/2,j+1}) \quad (8)$$
$$v_{i+1/2,j+1/2}=\frac{1}{2}(v_{i,j+1/2}+v_{i+1,j+1/2})$$

It may be noticed that as soon as pressures are known for all the cells, then equations (6) and (7) are immediately appropriate for the calculation of velocities. However it is tremendously time consuming to obtain the pressure field by iteration. Generally, the vorticity equation is used to obtain the velocity field independent of the pressure field. The finite difference approximation to the vorticity is,

$$\omega_{i+1/2,j+1/2}=\frac{u_{i+1/2,j+1}-u_{i+1/2,j}}{\delta x}-\frac{v_{i+1,j+1/2}-v_{i,j+1/2}}{\delta y} \quad (9)$$

Equations (6) and (7) can be combined to obtain an expression for $\omega_{i+1/2,j+1/2}$ which, like the differential equation, is independent of the pressure field. Therefore, the velocity field can be obtained by solving the vorticity equation (9). However, this equation has a great limitation when the problems are applied to 3-dimensional cases because the vorticity equation can not be applicable for 3-dimensional problems.

To attain the numerical scheme independent of dimensions, the penalty function approach is used to eliminate the pressure variable in governing equations. The continuity equation is perturbed in order to replace the pressure terms in the Navier-Stokes equations. The perturbed equation is represented by,

$$\frac{\partial u}{\partial x}+\frac{\partial v}{\partial y}=-\varepsilon P \quad , \quad (10)$$

where ε is typically between 10^{-5} and 10^{-9}. Physically, this can be treated as the flow of a very slightly compressible fluid. Equation (10) is now substituted to equations (2) and (3), then full velocity fields in each cell can be obtained. When the calculated velocity fields satisfy the continuity requirement, the next time step will be proceeded. This is so called modified Solution Algorithm-Volume of Fluid (MSOLA-VOF) method.

MSOLA-VOF has a great advantage over the SOLA-VOF in CPU times, because former requires calculation of velocity field only whereas latter needs the time-consuming iterative solution between velocity field and pressure field associated with vorticity calculation. Generally, the amount of CPU time requirement of the SOLA-VOF is order of magnitude larger than that of MSOLA-VOF due to iterative procedure between the variables.

2. 1 Boundary Conditions

Various boundary conditions may be applied at the wall of the computing mesh. In this pater, two boundary conditions, free-slip and non-slip, are used.

- A free slip boundary represents an axial centerline or a plane of symmetry or a nonadhering surface that exerts no drag upon the fluid. The normal velocity vanishes at the wall and there is no gradient in tangential velocity. This is represented with respect to a Eulerian fixed grid as,

$$u_{i,j}=0 \quad \text{at vertical wall.} \quad (11)$$
$$v_{i,j}=v_{i+1,j}$$

- A non-slip boundary condition represents an adhering surface that exerts drag upon the fluid. This is accomplished by forcing the tangential velocity to zero at the boundary. This is represented as,

$$u_{i,j}=0 \qquad \text{at vertical wall.} \qquad (12)$$
$$v_{i,j}=-v_{i,j}$$

2.2 Stablilty Criterion

Numerical analysis often cuases high frequency oscillations in space, time and both. This behavior is usually referred to as a numerical instability. To prevent the numerical instability, the choice of the time increment must be governed by several restrictions. First, material can not move through more than one cell in one time step because the difference equations assume fluxes only between adjacent cells.

$$\delta t<min\left(\frac{\delta x_i}{|u_{ij}|},\frac{\delta y_i}{|v_{ij}|}\right) . \qquad (13)$$

where the minimum is with respect to every cell in the mesh.

Second, momentum must not diffuse more than approximately one cell in one time step. A linear stability theory implies the limitation as,

$$\nu\delta t<\frac{1}{2}\frac{\delta x_i^2\delta y_j^2}{\delta x_i^2+\delta y_j^2} \qquad (14)$$

Equations (13) and (14) are used to adjust the time step in each time calculation.

3. Volume of Fluid Method

To simulate the filling process or free surface movements, it is necessary to trace the fractional volume of the fluid at the free surface. In MSOLA-VOF, the system is first divided into a number of cells, then a function $F(x, y, t)$ is defined at every cell which value is unity in a region which fluid is occupied and value of zero elsewhere. Cells with F values between zero and one contain a free surface (Figure 2).

The time dependent variable F is governed by equation in the domain where $0<F\leq 1.0$,

$$\frac{\partial F}{\partial t}+u\frac{\partial F}{\partial x}+v\frac{\partial F}{\partial y}=0 . \qquad (15)$$

By combining equations (1) and (15), the VOF function F can be written as,

$$\frac{\partial F}{\partial t}+\frac{\partial Fu}{\partial x}+\frac{\partial Fv}{\partial y}=0 . \qquad (16)$$

The integration of the equation (16) over a computational cell can be reduced to fluxes of F across the cell faces. The amount of volume transported in and out of a cell is calculated after the velocity field is obtained in equations (6) and (7). Therefore, it is relatively easy to obtain F values as time progresses.

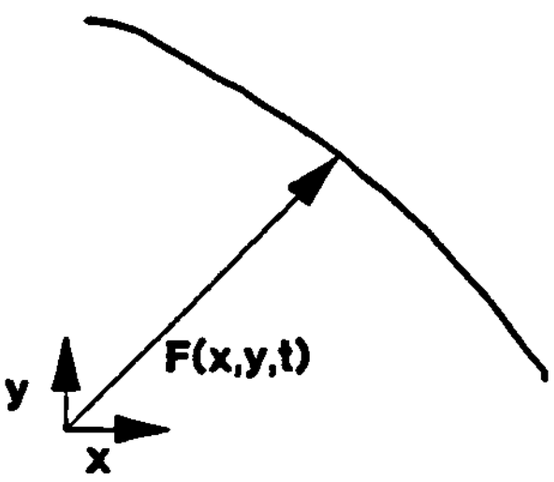

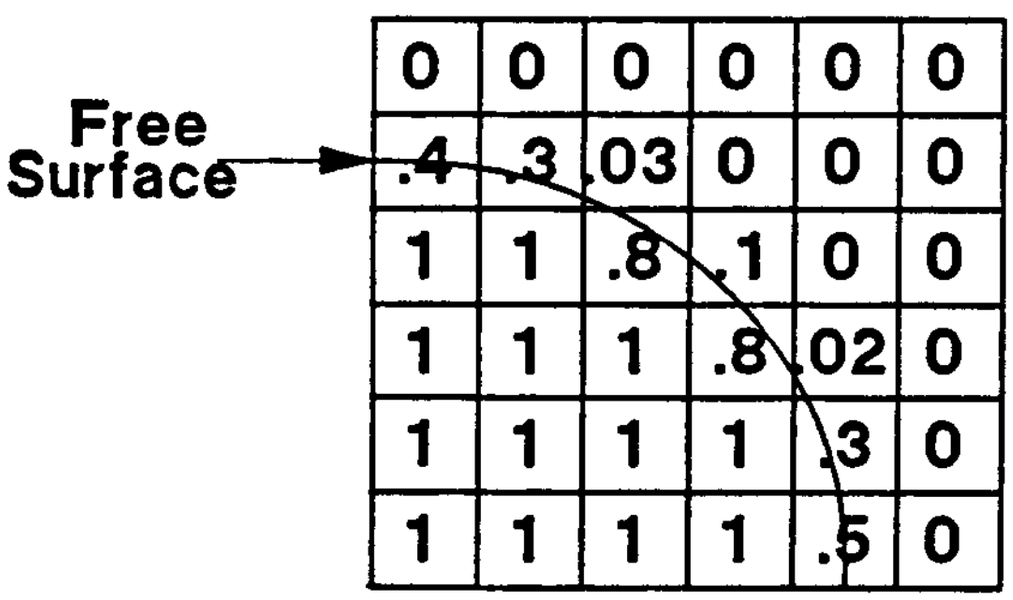

Figure 2. Fluid domain obtained with VOF function (F) using the MSOLA-VOF method.

4. Results and Discussions

Fluid flow in the mold cavity during the

filling process is highly transient ; the amount of fluid volume and location of the free surface change rapidly. Calculation of the location of free surface and the internal velocity movements play a significant role in characterizing the segregation of the castified material. To understand the velocity distributions and the free surface movements in the mold cavity, two cases are simulated.

The first case is a horizontal casting shown in Figure 4(d). The fluid is injected through the ingate on the left side of cavity with inflow velocity of 10*cm/sec*. The cross section of the mold is assumed to be infinite, so it can be treated as a 2-dimensional flow

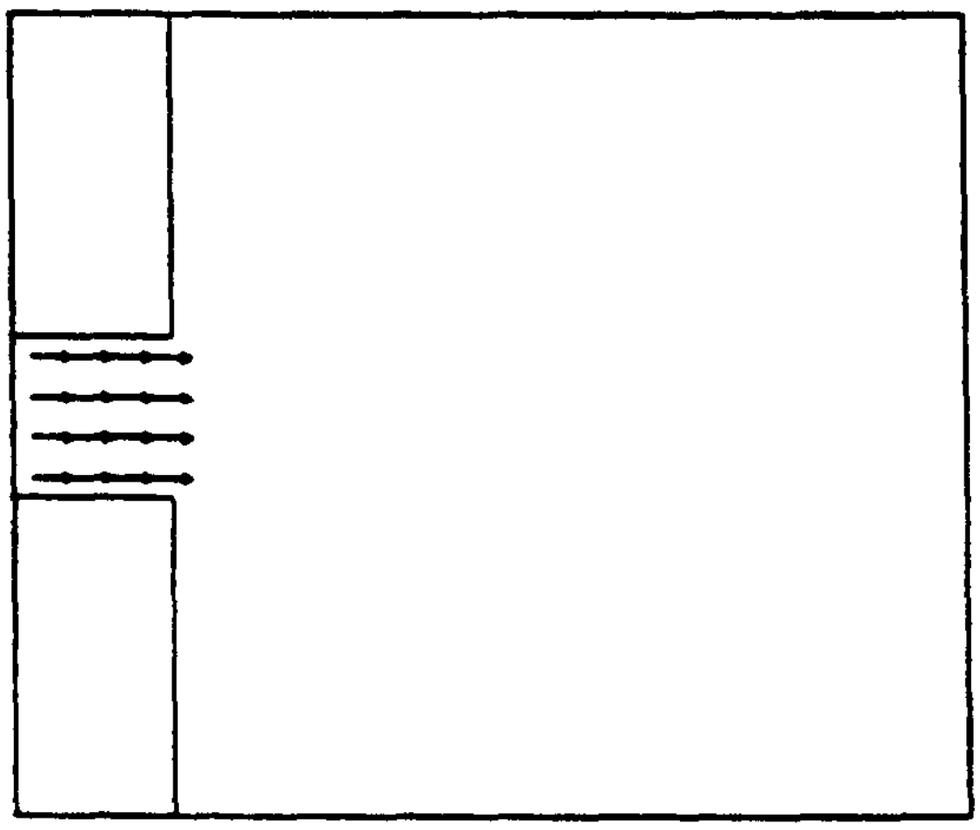

(a) t=0 sec

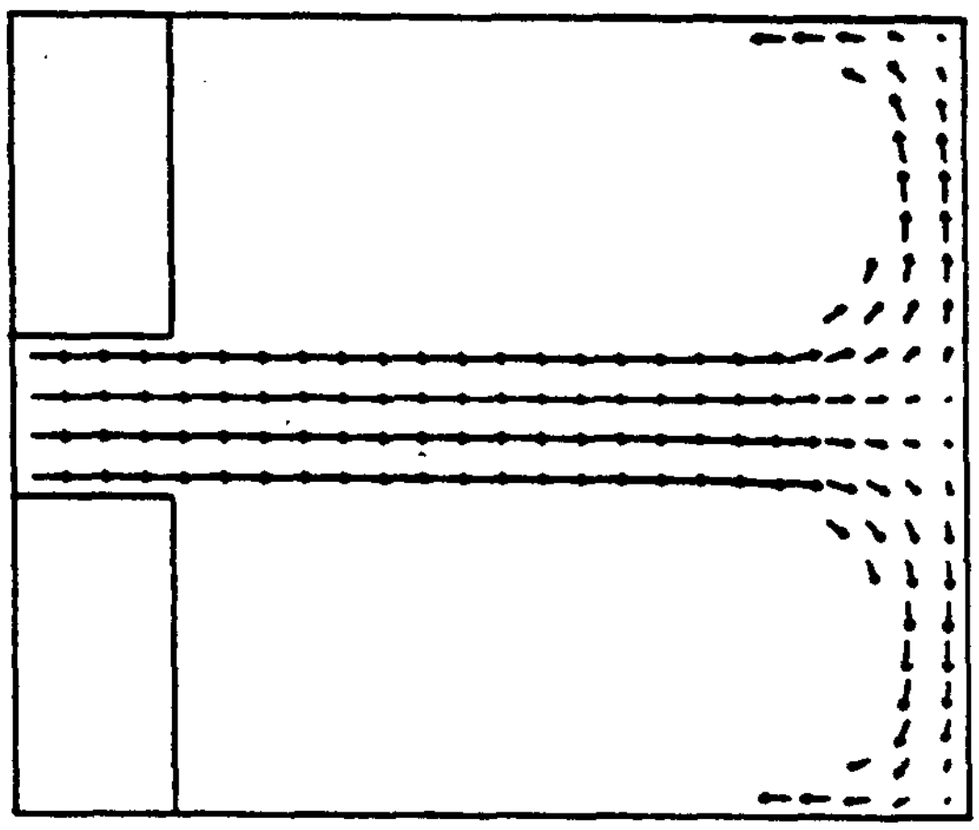

(b) t=3 sec

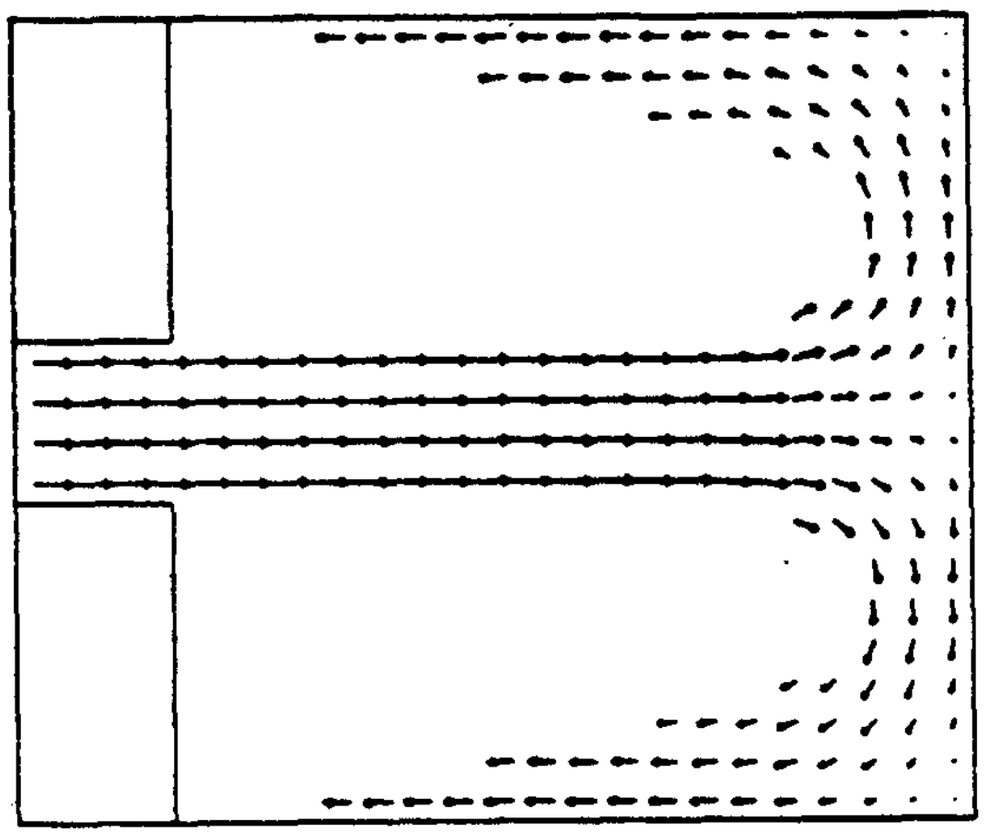

(c) t=4.5 sec

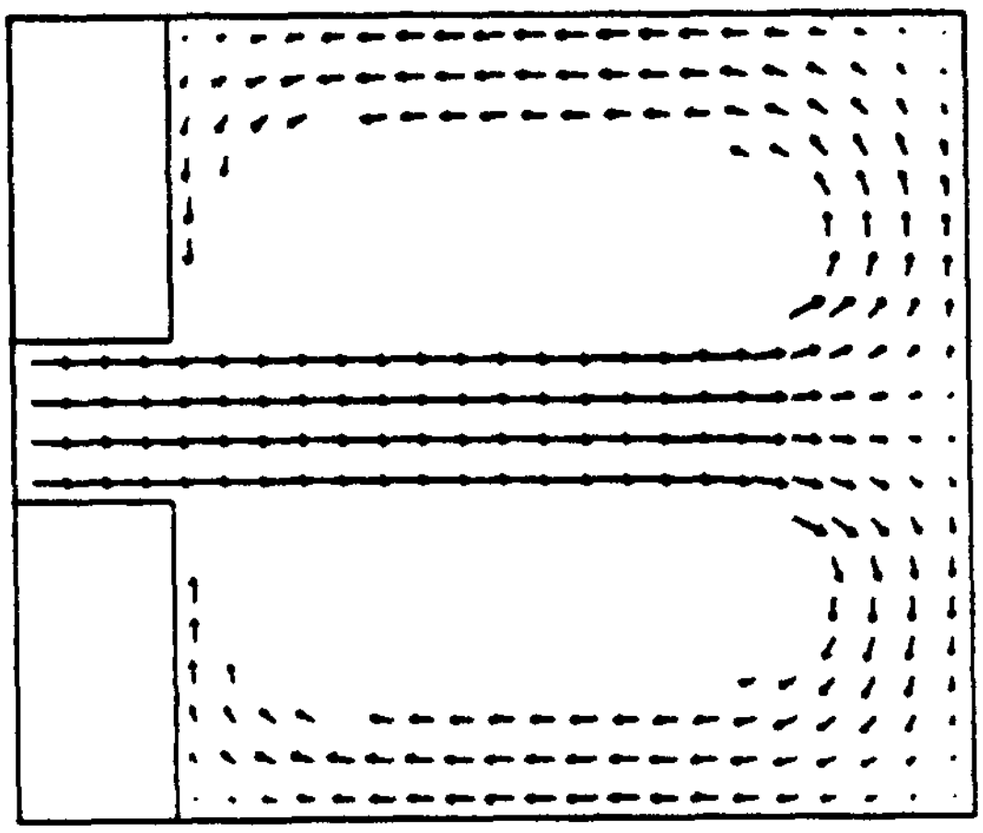

(d) t=6 sec

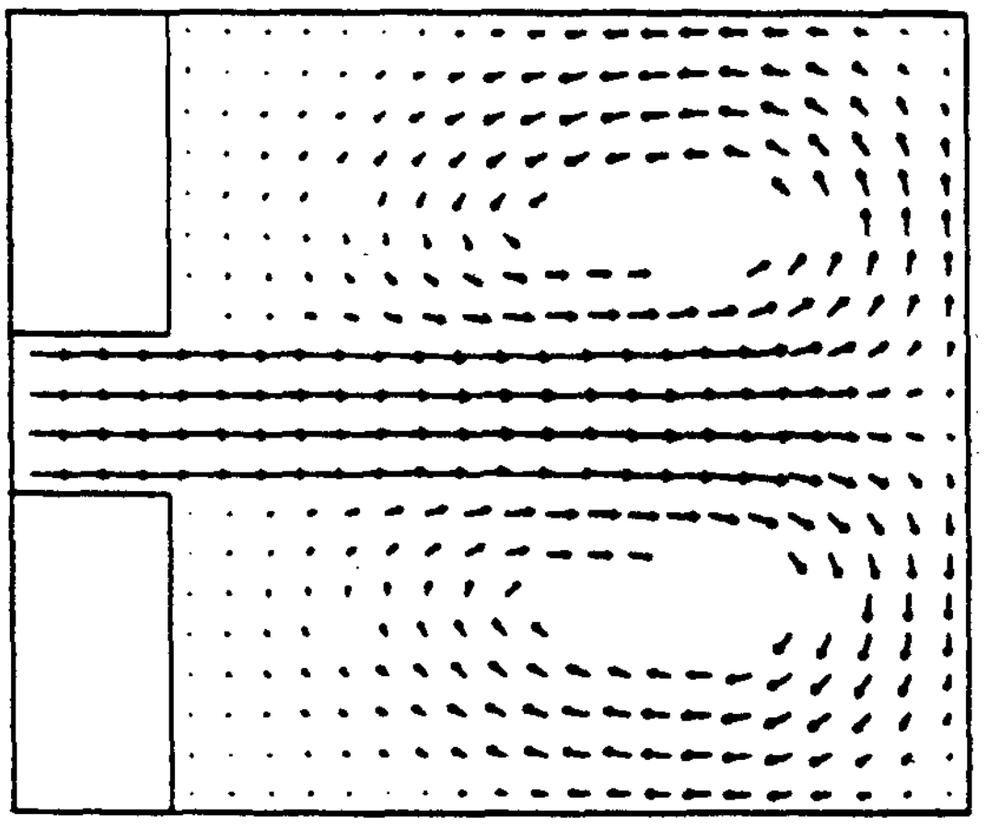

(e) t=9 sec

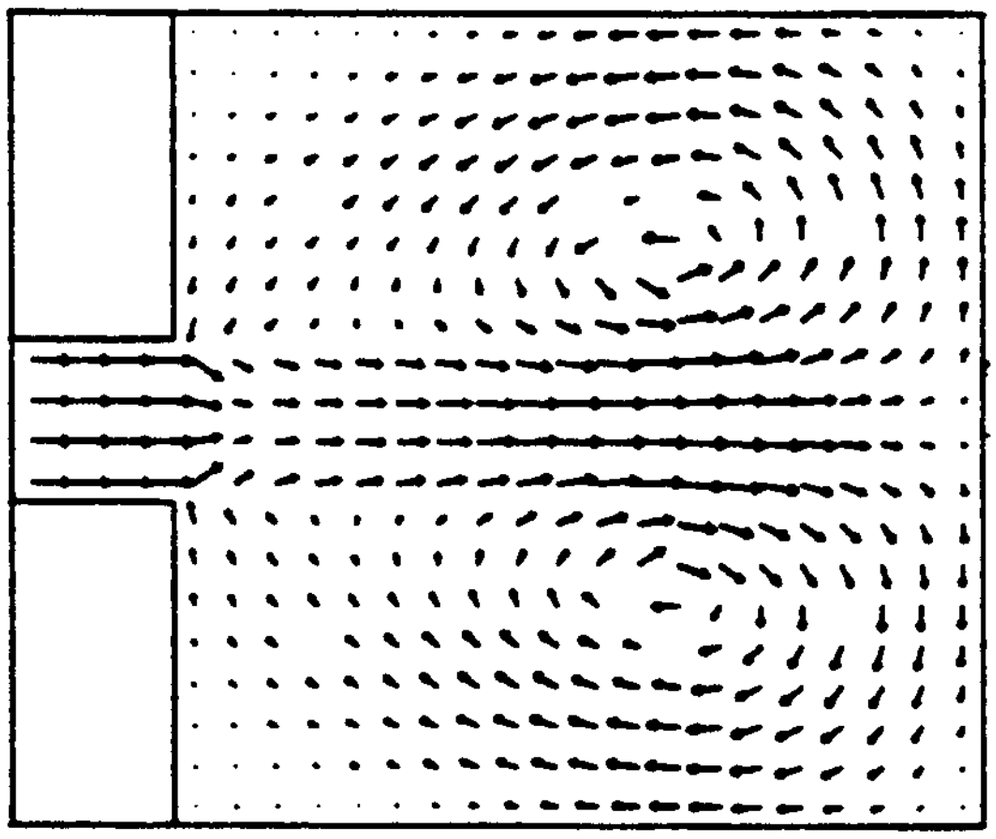

(f) t=10.5 sec

Figure 3. The fluid pattern in the horizontal casting at various time intervals(without gravity force).

phenomenon. The kinematic viscosity and the gravity are set, $\nu=0.1m^2/sec$ and $g=9.8m/sec^2$, respectively.

In the beginning, the fluid is about to move into the cavity. As the simulation progresses, the molten metal enters in the direct fashion and hits the wall on the right side. Due to the momentum changes at the right wall, it changes the flow direction to the left. 6 seconds later from the start, the left running flow meets the inflow stream and forms two air pockets on the upper and lower side of ingating fluid stream (Figure 3

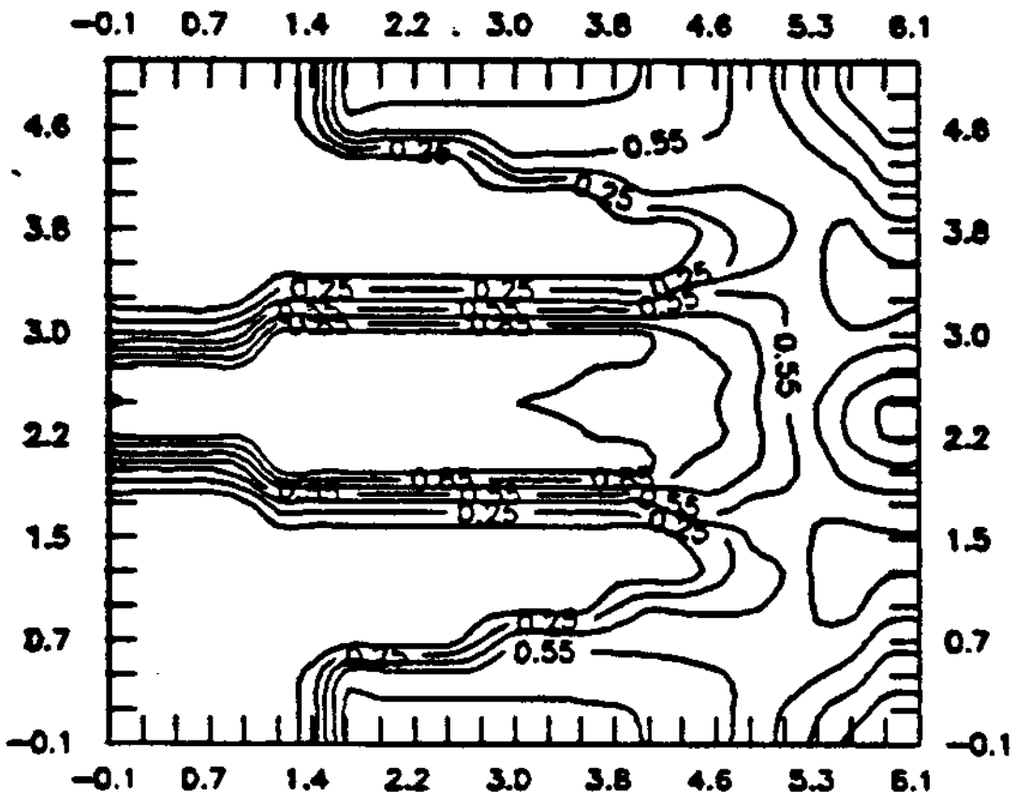

(a) t=4.5 sec

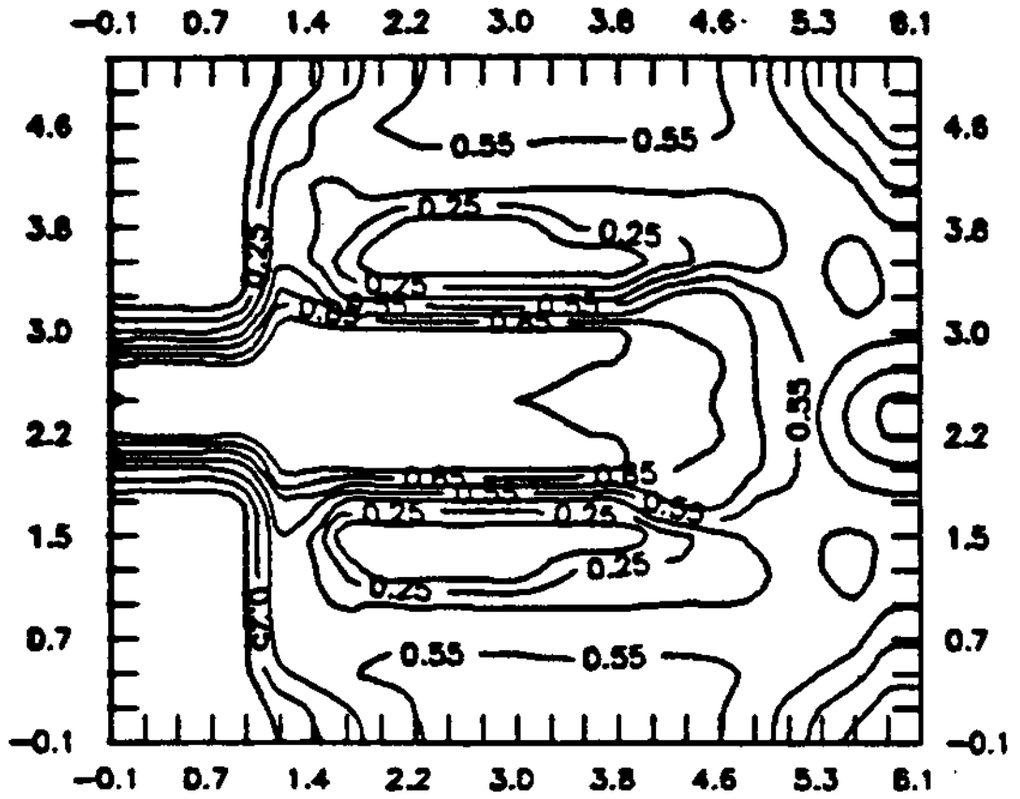

(b) t=9 sec

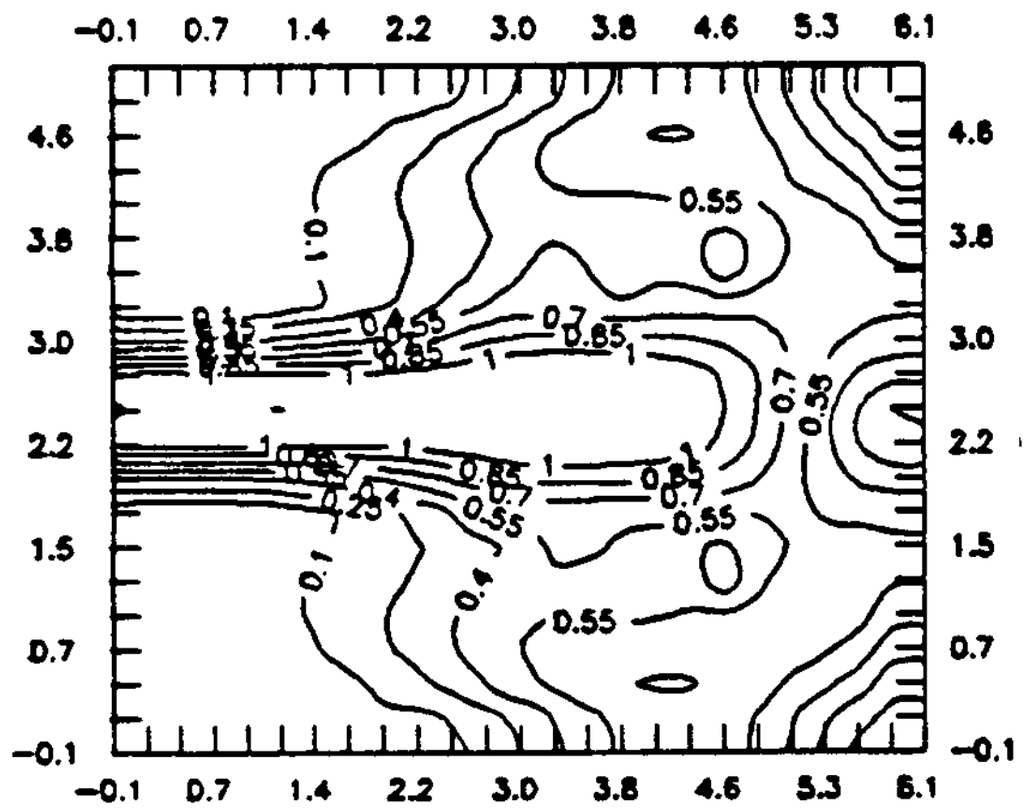

(c) t=10.5 sec

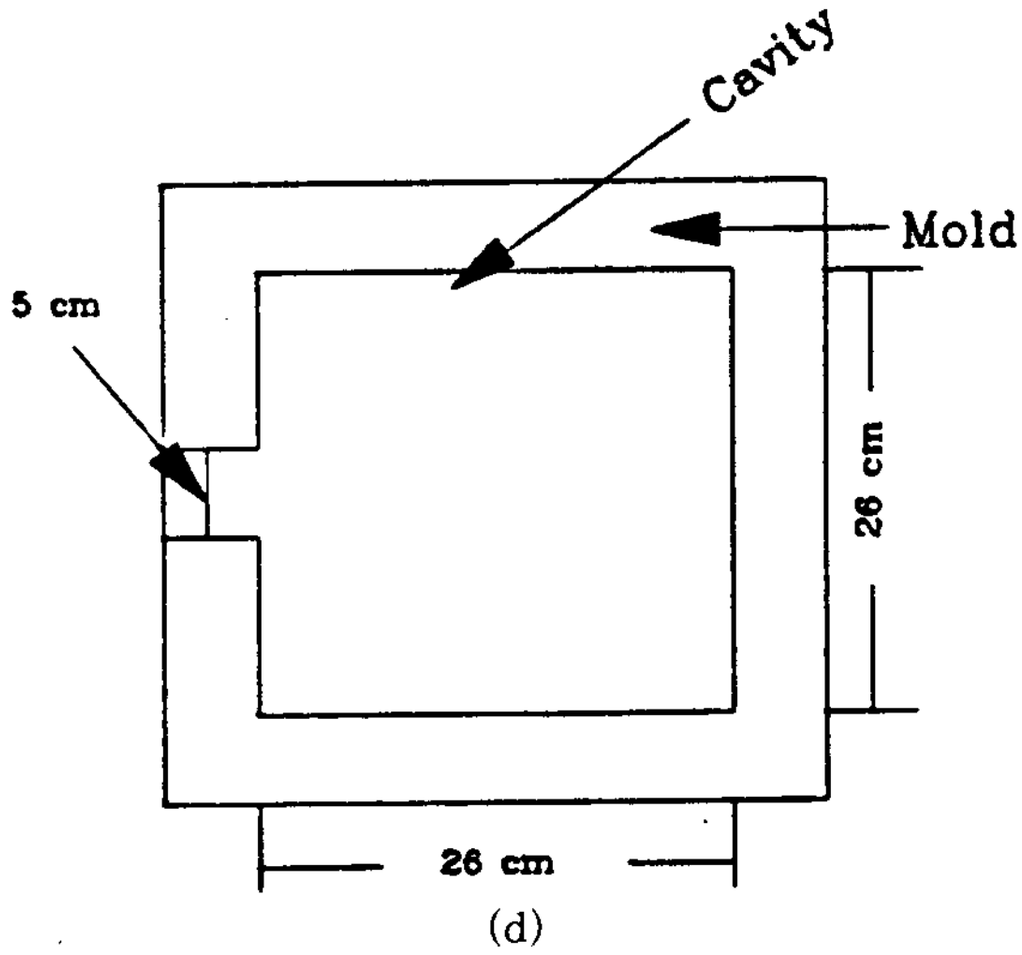

(d)

Figure 4. The iso-velocity lines at various time intervals and schematic of the casting domain.

(d)-(e)). As time reaches 10.5 second, the cavity is filled with molten metal shown in Figure 3(f). When compared with SOLA-VOF method,[13] these numerical results show good accuracy.

To understand the internal velocity distributions some cases are selected from calculated results and are displayed in Figure 3. Figure 4 shows the iso-velocity line. As depicted in Figure 4, the strong velocity fields are found in the center of cavity at the beginning stage of the process. As the time progresses, the strong velocity fields are maintained at the center and transient velocity patterns are exhibited on the upper and lower side of the cavity. Figure 4(c) represents the final iso-velocity line. It is found that the magnitude of the velocity is larger on the right side of the cavity than on the left side of the cavity.

The second case is a vertical casting shown in Figure 5. The cross section of the casting domain is assumed to be infinite that the flow phenomenon can be treated as the two dimensional case. The molten metal is seen at the ingate and ready to enter the cavity with ingate velocity of $10cm/sec$. At 3 second, the front of incoming fluid hits the wall on the right and jumps up. As the time progresses, the molten metal hits the ingate

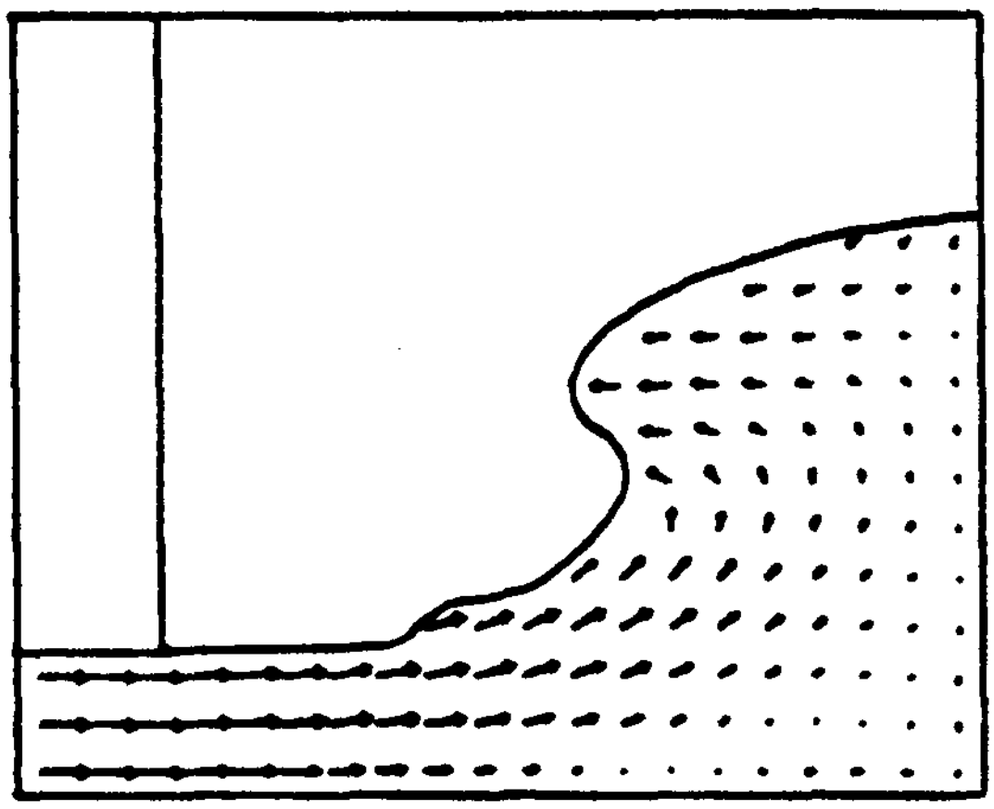

(b) t=4.5 sec

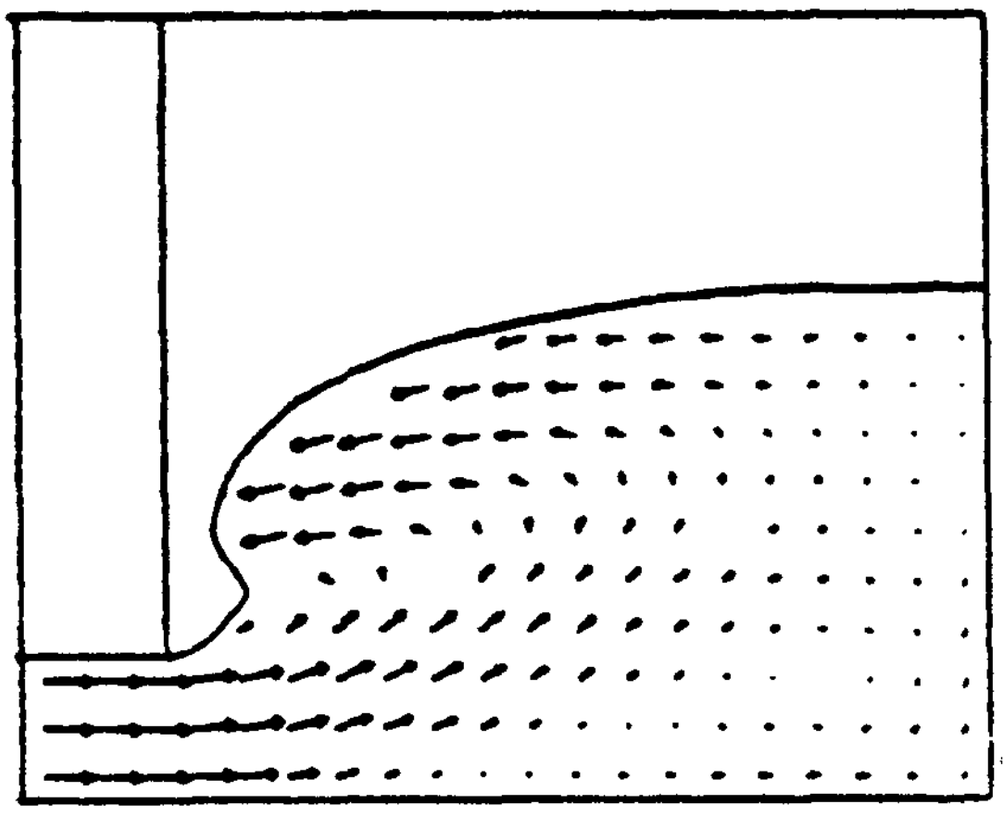

(c) t=5.5 sec

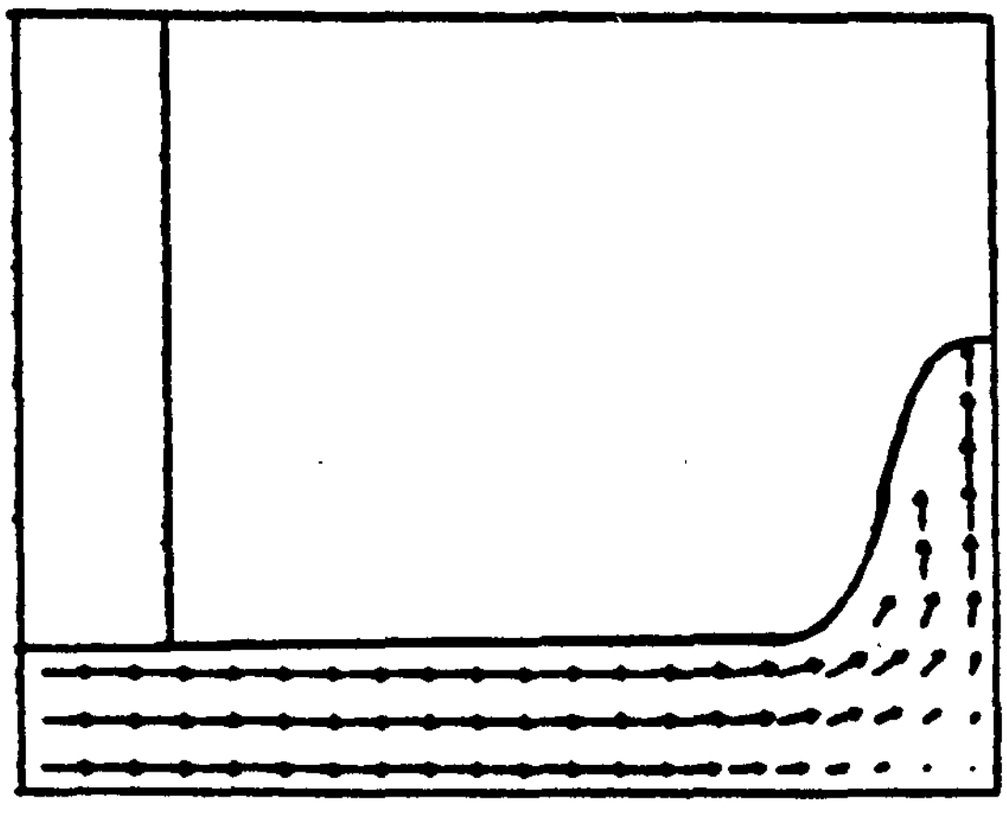

(a) t=3 sec

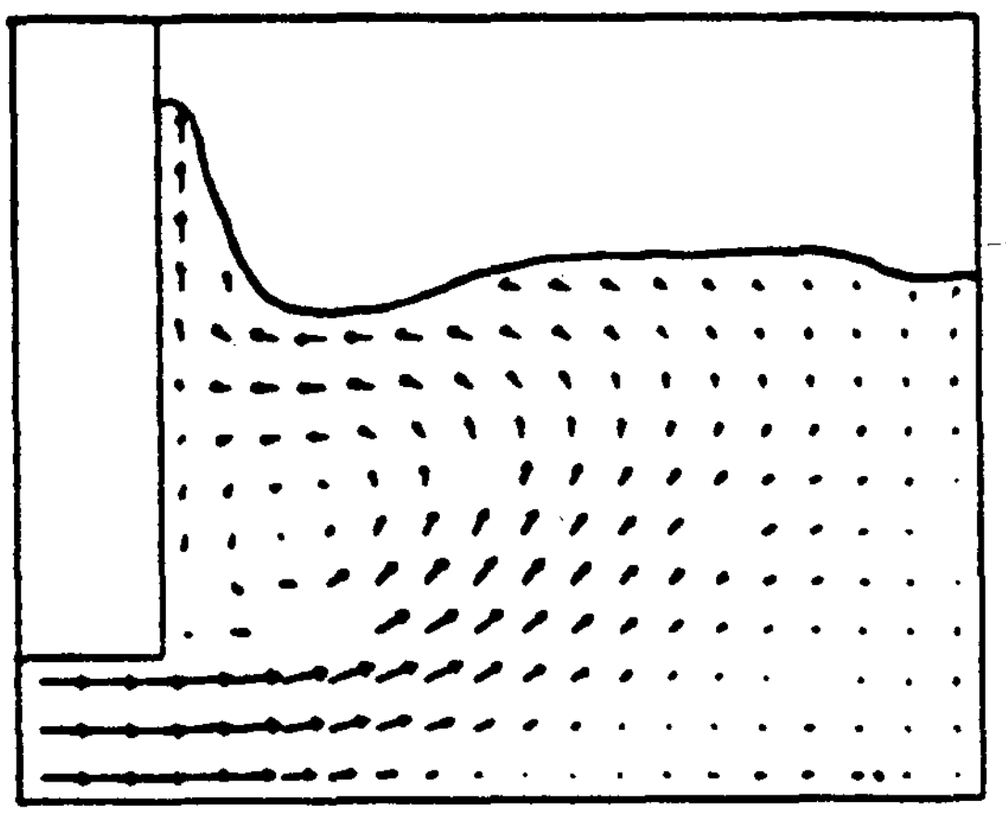

(d) t=6.5 sec

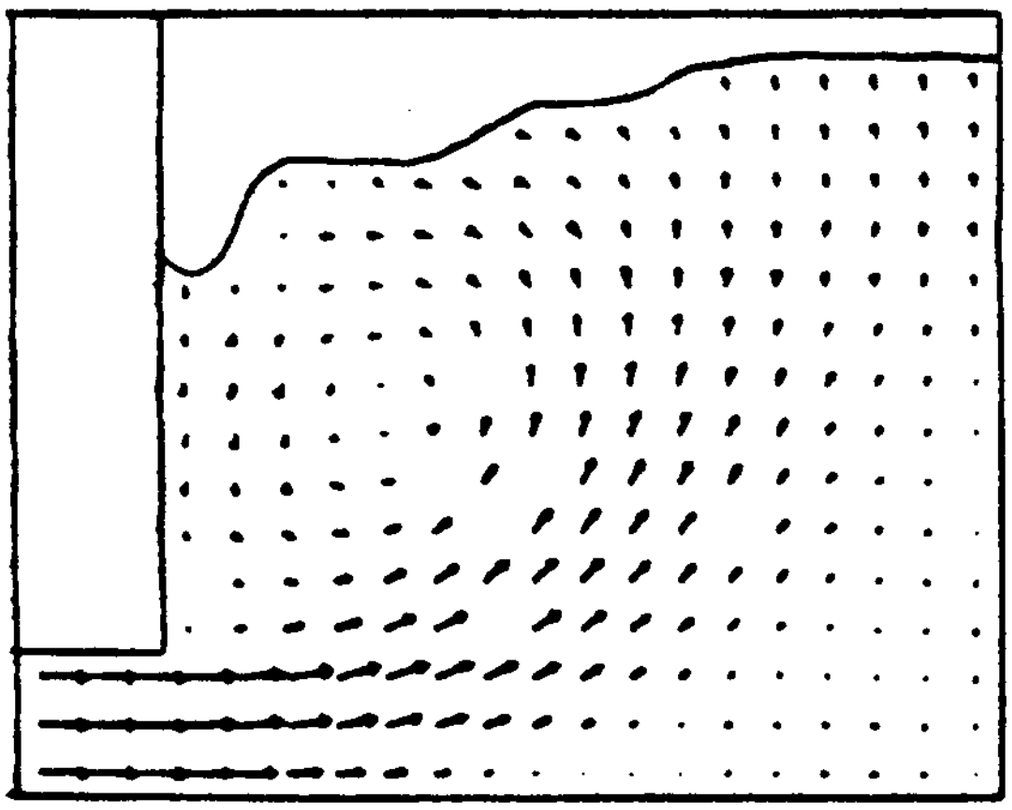

(e) t=8 sec

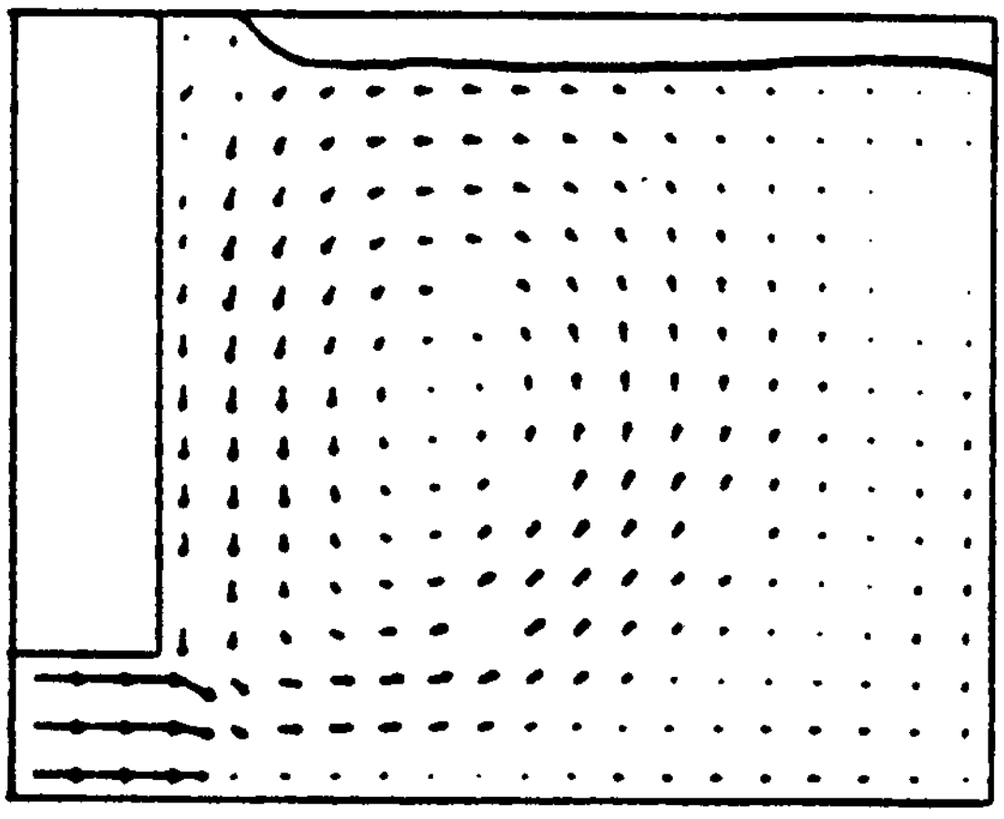

(f) t=8.5 sec

Figure 5. The fluid patterns in the vertical casting at various time intervals(with gravity force).

flow and climbs upward direction to fill up the cavity. A vortex is generated near the ingate due to the flow direction changes and ingate flow.

Several time steps of vertical casting are examined to understand the magnitude of velocity during the mold filling process. Figure 6 shows the iso-velocity contours. As depicted in Figure 6, the strong velocity field maintains its effect in diagonal direction due to the boundary layer growth and the confinement of the cavity. Note that the velocity scales are reduced to the one tenth of the originally calculated results.

To validate the present algorithm associated with penalty approach, broken dam problem which is the most typical illustration of free surface movement is considered. In-

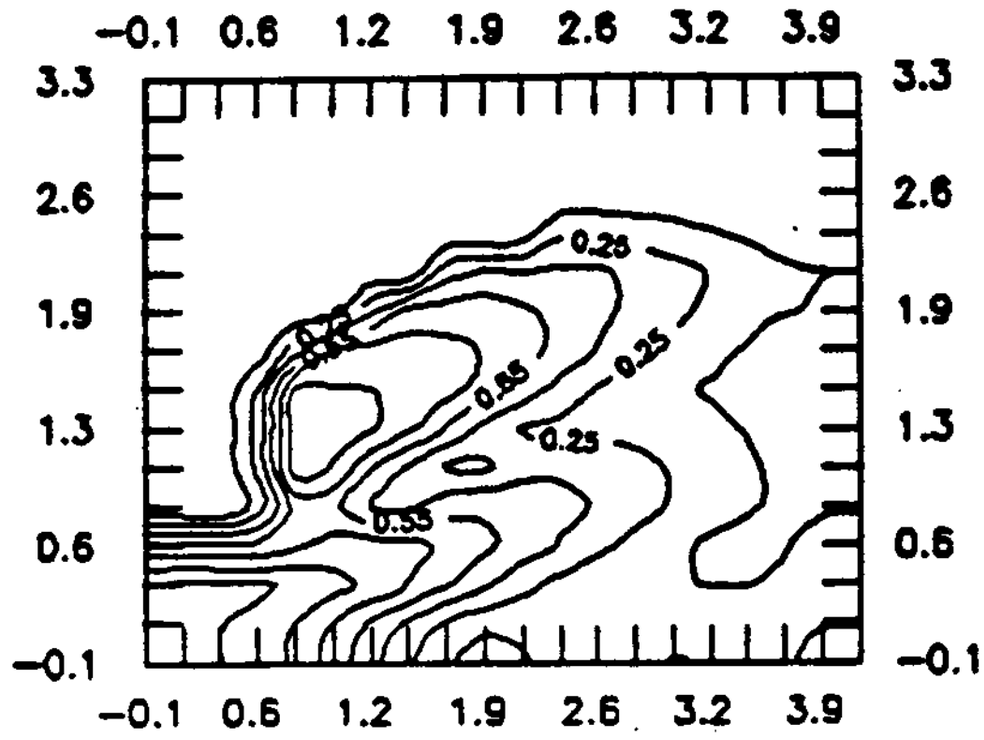

(a) t=5.5 sec

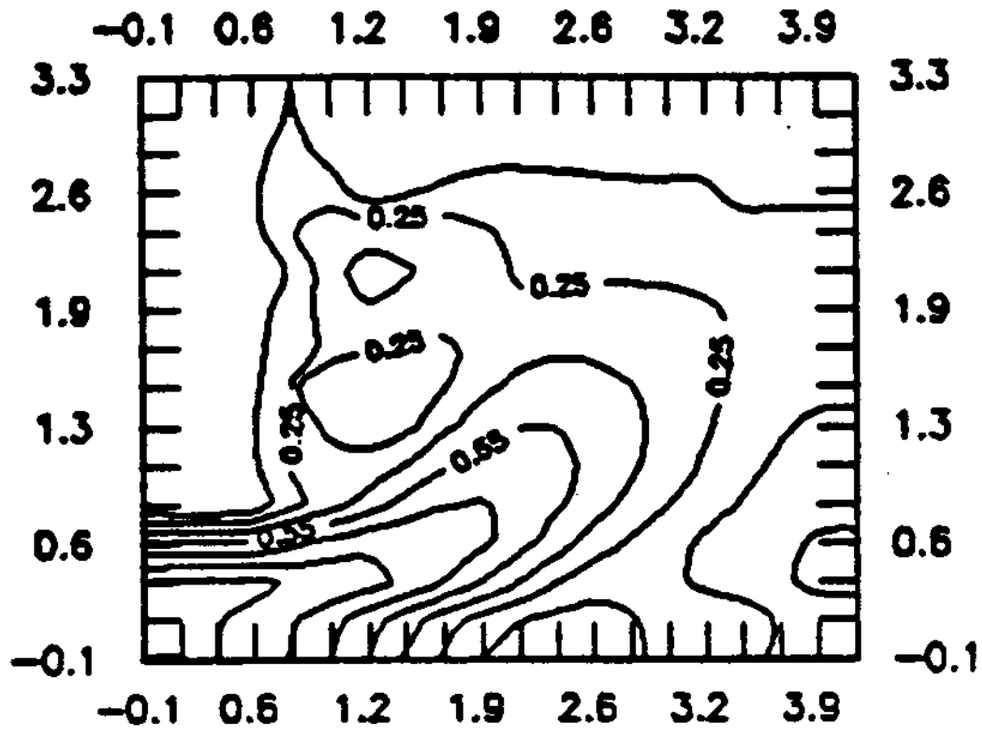

(b) t=6.5 sec

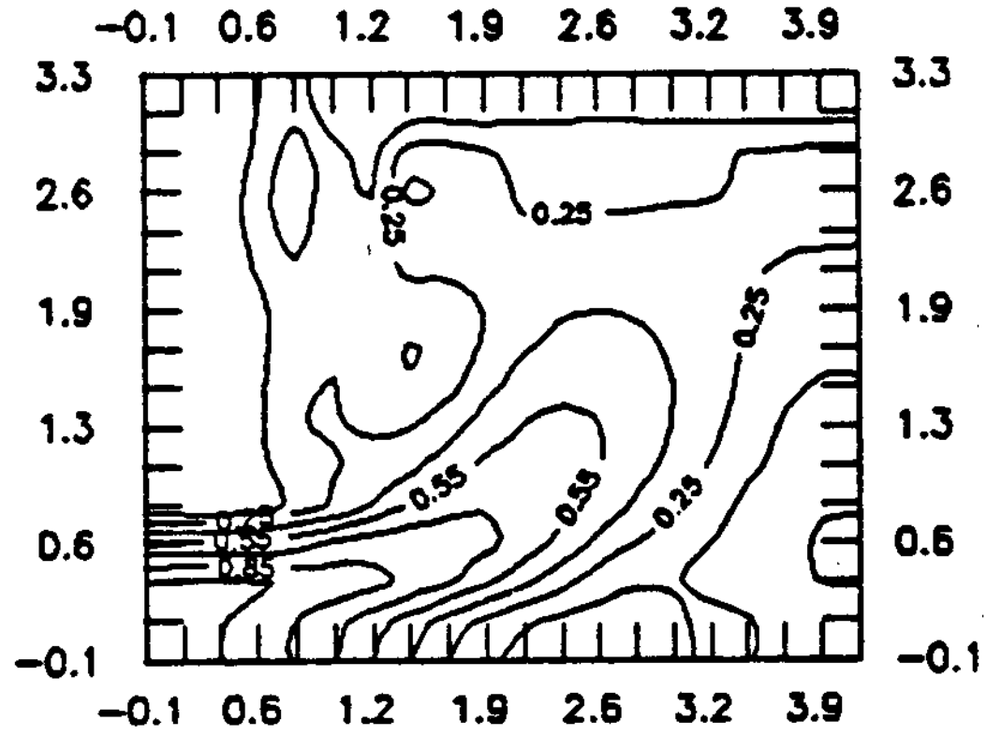

(c) t=8.5 sec

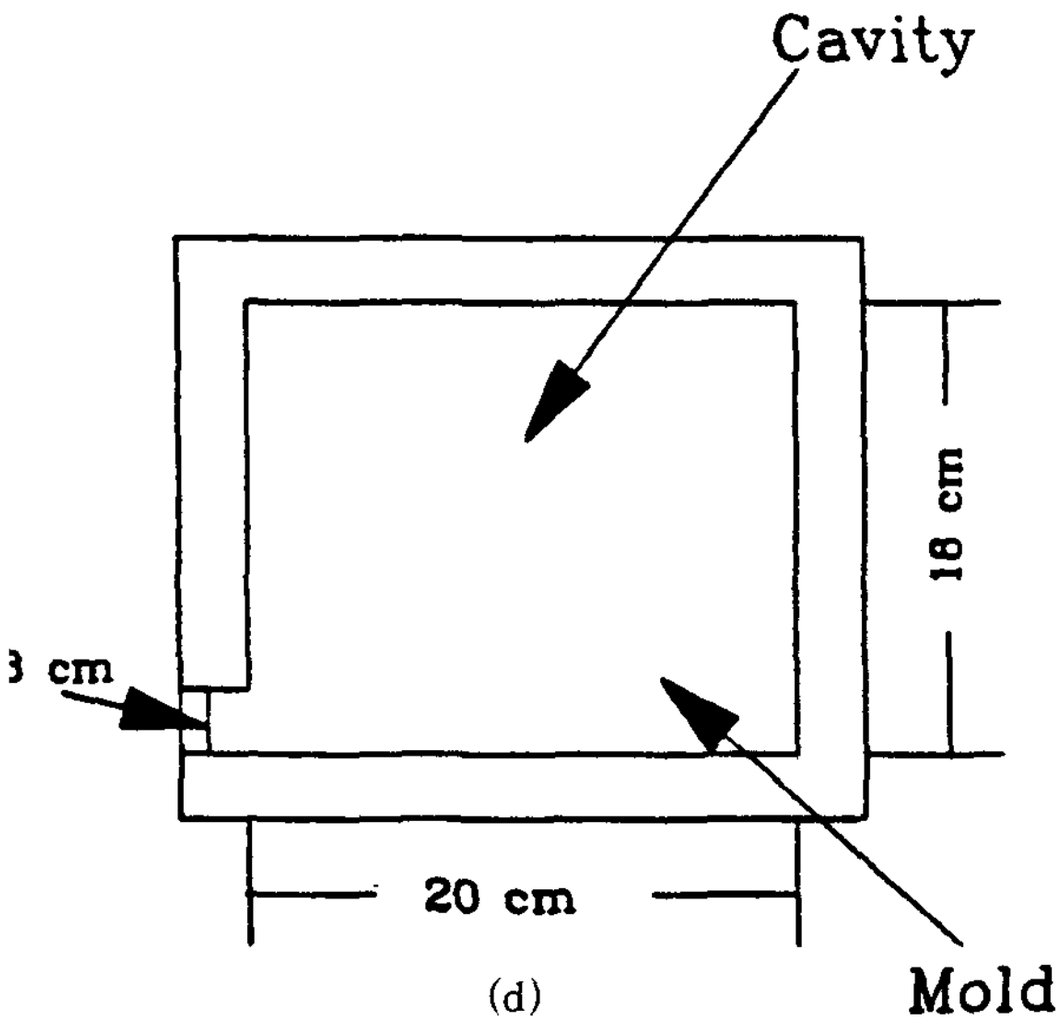

(d)

Figure 6. The iso-velocity lines at various time intervals and schematic of the casting domain.

itially, a rectangular column of water is confined between the two vertical walls (Figure 7). At the beginning of the calculation, the right wall is removed to allow water flow. Experimental results for this problem have been reported[9] for the position of leading edge of water vs time. The comparison between the MSOLA-VOF and experimental results are shown in Figure 3 and it demonstrates the accuracy of MSOLA-VOF.

In conclusion, it is important to notice that segregation of the castified materials is dependent of the internal velocities[14), 15)] because the convective terms in governing equations, $(u \cdot \nabla u)$ and $(u \cdot \nabla T)$, play a magnificent role in characterizing the solidfication phenomena. Therefore, the initial velocity distributions caused from the filling process must be considered to understand the exact segregation behaviors. Comparing MSOLA-VOF method with other algorithms handling free surface flow problems, MSOLA-VOF method gives relatively high accuracy. In addition, this algorithm can be applicable to 3 dimensional cases and to the problems with thermal property changes during mold filling process.

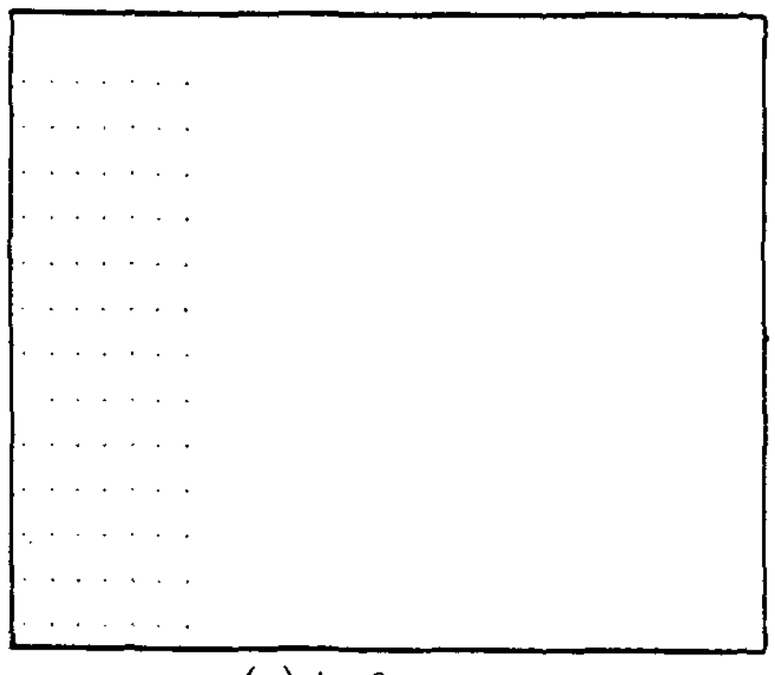

(a) t=0 sec

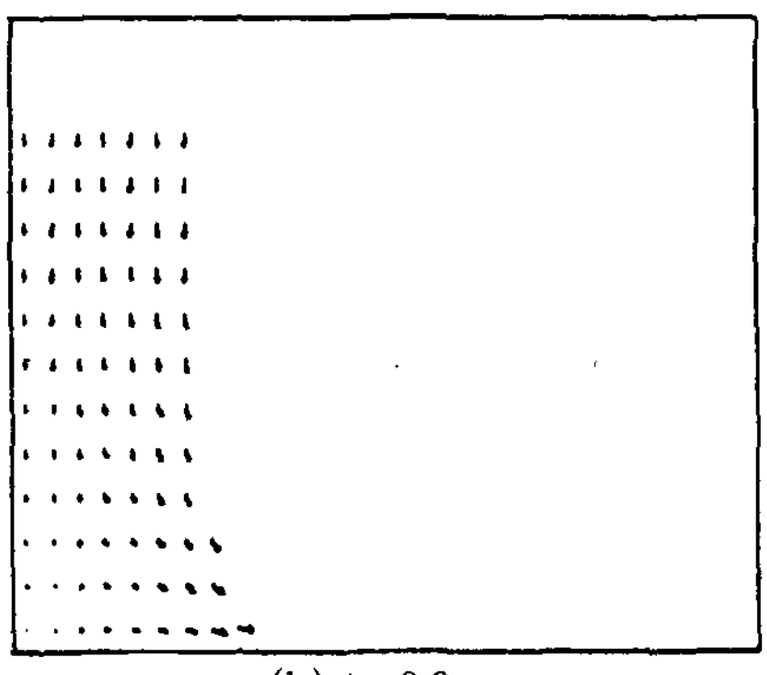

(b) t=0.2 sec

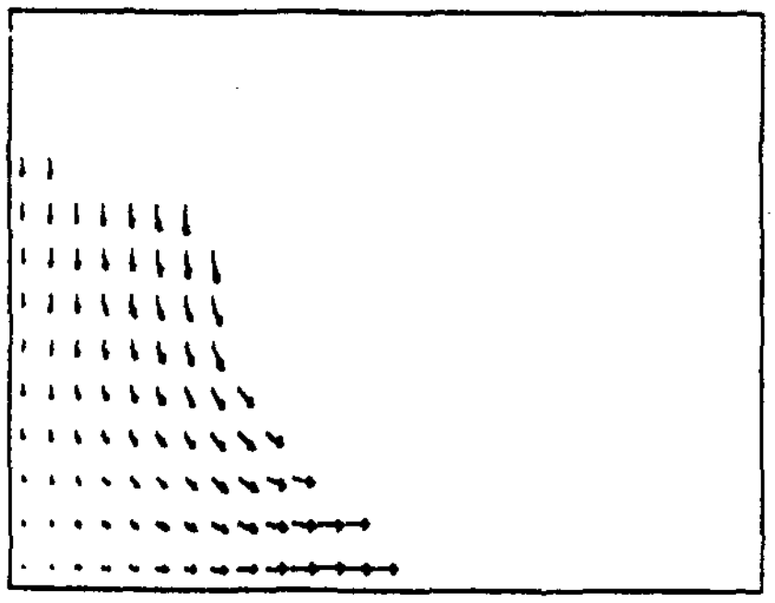

(c) t=0.5 sec

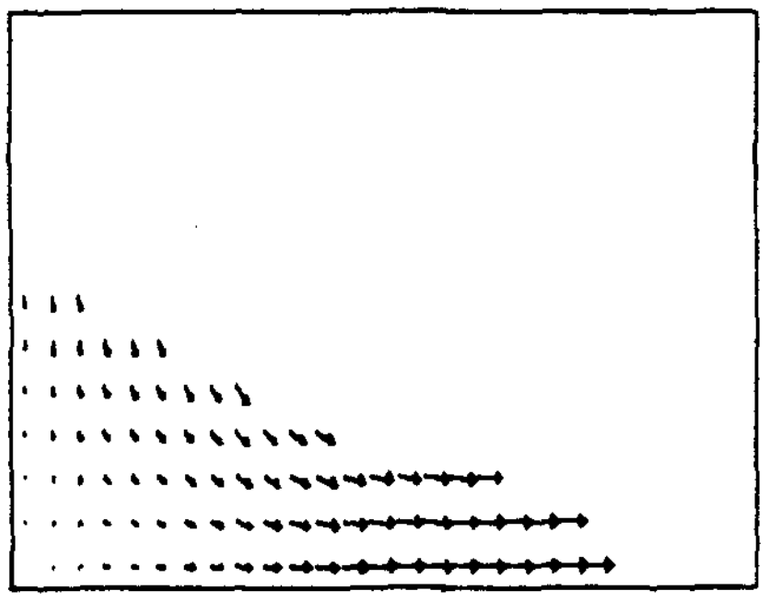

(d) t=1.0 sec

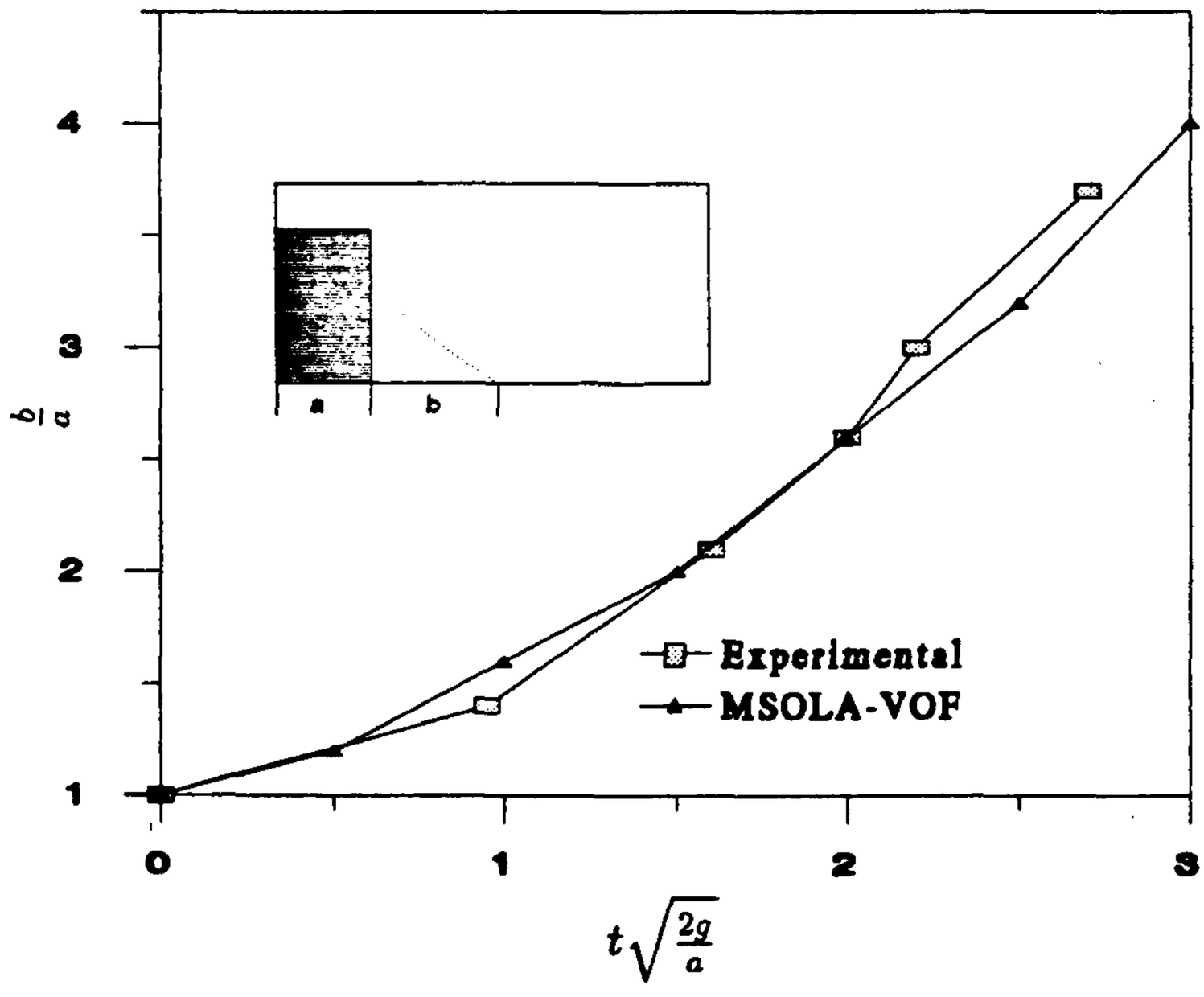

Figure 7. The fluid patterns ((a)～(d)) and comparison of calculated results vs. experimental data(e).

Nomenclature

F : Volume of fluid
g_x : Body force in x-direction
g_y : Body force in y-direction
t : Time
u : Velocity in x-direction
v : Velocity in y-direction
x : x-axis
δx : Space of x cell
y : y-axis
δy : Space of y cell
P : Pressure
ν : Kinematic viscosity
ε : Penalty value
ω : Vorticity

References

1. H.M. Ettouney and R.A. Brown, "Finite Element Methods for Steady Solidification Programs", J. of Comp, Phys., Vol. 49, 1983, pp. 118-124.
2. V.R. Voller, N.C. Markatos and M. Cross, "An Enthalpy Method for Convection Diffusion Phase Changes", Int. J. Num. Meth. Engng., Vol. 24, 1987, pp. 271-284.
3. V.R. Voller and C. Prakash, "A Fixed Grid Modeling Methodology for Convection Diffusion Mushy Region Phase-Change Problems", Int. J. Heat Mass Transfer, Vol. 30, 1987, pp. 1709-1719.
4. C. Gau and R. Viskanta, "Melting and Solidification of a Metal System in a Rectangular Cavity", Int. J. Heat Mass Transfer, Vol. 27, 1984, pp. 113-123.
5. K.V. Palglthivarthi and P.V. Desai, "Modeling Thermosolutal Convection in Binary Alloy Solidification", Met. Society, AIME, 1986, pp. 121-128.
6. C. Beckermann and R. Viskanta, "Effect of Solid Subcooling on Natural Convection Melting of a Pure Metal", Tran. of the

ASME. 1989, pp. 416-424.
7. J.E. Welch, F.H. Harlow, P.J. Shannon and B.T. Dally, "The MAC Method-A Computing Techniques for Solving Viscous, Incompressible, Transient Fluid Flow Problems Involving Free Surfaces", Technical Report LA-3425, Los Alamos Scientific Laboratory, 1965.
8. A.A. Amsden and F.H. Harlow, "The SMAC Method, A Numerical Technique for Calculating Incompressible Flows", Technical Report LA-4370, Los Alamos Scientific Laboratory, 1970.
9. B.D. Nichols, C.W. Hirt and R.S. Hotchkiss, "SOLA-VOF, A Solution Algorithm for Transient Fluid Flow with Multiple Free Boundaries", Technical Report LA-8355, Los Alamos Scientific Laboratory, 1980.
10. C.W. Hirt and B.D. Nichols, "A Computational Method for Free Surface Hydrodynamics", ASME Pressure Vessels and Piping Conference, San Francisce, 1980,
11. B.D. Nichols, C.W. Hirt and R.S. Hotchkiss, "A Fractional Volume of Fluid Method for Free Boundary Dynamics", Technical Report LA-UR-80-1631, Los Alamos Scientific Laboratory, 1980.
12. W.S. Hwang and R.A. Stoehr, "Fluid Flow Modeling for Computer Aided Design of Casting", J. Met., Vol. 35, 1983, pp. 22-30.
13. H.J. Lin and W.S. Hwang, "Combined Fluid Flow and Heat Transfer Analysis for the Filling of Casting", AFS Trans., Vol. 96, 1988, pp, 447-458.
14. J.H. Kim, "Simulation of Microsegregation during Binary Alloy Solidification," Ph.D. Thesis, Georgia Institute of Technology, 1990.
15. J.H. Kim, I.C. Lim and C.W. Meyers, "Simulation of Solid-Liquid Interface Behaviors during Solidification," J. Metal, (will appear in 1992).